7-14-2015

Using peptides to examine the interaction interface between Aspartate transcarbamoylase and Dihydroorotase in pyrimidine biosynthesis in Aquifex aeolicus

Nouf Alyami

Using Peptides to Examine the Interaction Interface between Aspartate transcarbamoylase and Dihydroorotase in Pyrimidine Biosynthesis in *Aquifex aeolicus*

by

Nouf Alyami

Thesis

Submitted to the Department of Chemistry

Eastern Michigan University

in partial fulfillment of the requirements

for the degree of

MASTER OF SCIENCE

in

Chemistry

Thesis Committee:

Hedeel Evans, Ph.D., Chair

Deborah Heyl-Clegg, Ph.D.

Vance Kennedy, Ph.D.

July 14, 2015

Ypsilanti, Michigan

DEDICATION

This work is dedicated to my parents, without whose support it would not have been possible.

A special feeling of gratitude to my loving siblings Nada, Bayan, and Bader whose laughter is like music to my soul.

Also, I dedicate this work to my two grandmothers whose hearts are full of prayers for me.

I dedicate this work and give special thanks to my Father's friend, Waleed, whose words of encouragement and push for tenacity continue to ring in my ears.

I also dedicate this work to my best friend, Jomanah.

I dedicate my thesis to every member of my supportive family, and to my friends, for being there for me throughout the master's program.

Finally, I dedicate this work to the one whose life is a source of happiness for me.

ACKNOWLEDGMENTS

I would like to give my special thanks to my advisor Dr. Hedeel Evans, my committee chair, for her unlimited support and patience. Dr. Evans spared me a lot of her effort and knowledge, which has helped me in my research. I would also like to give my appreciation to my advisor, Dr. Deborah Heyl-Clegg, for her time and support during my research. I would like to record my appreciation for Dr. Vance Kennedy, for being a member of my thesis committee.

I would like to thank Dr. Ruth Ann Armitage, for the provision of electrospray ionization mass spectrometry. I also thank Dr. Jeffrey Guthrie for teaching me new experiments and skills. Of course, huge thanks to Dr. Timothy Brewer for being such a supportive advisor to graduate students.

I gratefully acknowledge all the faculty members of the chemistry department at Eastern Michigan University who provide me the benefit of their guidance and experience.

ABSTRACT

Aspartate transcarbamoylase (ATCase) and Dihydroorotase (DHOase) catalyze the second and third steps, respectively, in *de novo* pyrimidine biosynthesis. Both enzymes form an active complex (DAC) in *Aquifex aeolicus*, where loop A of DHOase interacts with a domain of ATCase. The main objective of this work is to determine the function of specific residues of loop A in DAC interactions and to alter the catalytic activities through disruption of the interface between the two enzymes from *A. aeolicus.* The ATCase and DHOase domains have been expressed in *Escherichia coli* and purified using affinity chromatography. The interface of the published three-dimensional structure of the non-covalently associated dodecamer of DHOase and ATCase from *A. aeolicus* was examined using bioinformatics, and a peptide was designed to block a specific hydrophobic region. In this work, several peptides have been synthesized by solid phase peptide synthesis (SPPS). Assays were conducted to determine the binding affinities of the peptides to the DHO-ATC complex.

TABLE OF CONTENTS

LIST OF TABLES

LIST OF FIGURES

CHAPTER 1: INTRODUCTION

Introduction

Cancer is a disorder which involves uncontrolled cell division, resulting in a destruction of body tissue. In the United States, cancer is the second highest cause for deaths, with nearly one in every four people falling victim to it. Based on the data provided by the American Cancer Society in its 2014 cancer incidence statistics, more than 1,500,000 new cancer cases and more than 500,000 cancer deaths were estimated.

How does cancer form? Each cell in the body has DNA that carries the cell's information. If the DNA becomes damaged, the cell will not function normally. Cancer starts when these abnormal cells start dividing uncontrollably,[1] and there are many mechanisms that these cancer cells employ to divide without any regulatory control.

Pyrimidine nucleotides have a major role in cell growth.[2,3] In cancer, *de novo* pyrimidine biosynthesis is upregulated. Thus, there is need for effective chemotherapeutic agents that act by targeting the enzymes that catalyze this pathway in the earliest steps.[4] Understanding the role of the pyrimidine pathway in the rapid growth of tumors can be achieved, in part, by understanding the process of pyrimidine *de novo* biosynthesis in prokaryotic cells. The analogous pyrimidine biosynthetic enzymes from the *A. aeolicus* bacteria are used as a model system because of their known homology with the mammalian counterparts. Targeting the enzymes involved in the second and third steps of this pathway in *A. aeolicus* may lead to the development of new drugs for cancer in the long run.

Pyrimidine Pathway

The pyrimidine pathway performs a major role in cell metabolism by activating the precursors of DNA and RNA, CDP-triacylglycerol, and phosphoglyceride, which are needed for assembling cell membranes, and the precursors needed for the glycosylation of proteins and the synthesis of glycogen by UDP-Glucose. Moreover, the uridine nucleotide, which is formed by pyrimidine biosynthesis,[2] regulates a different physiological process through extracellular receptors.[3] Pyrimidine synthesis has two different paths: the nucleotides can be reused by the salvage pathway, or they can be synthesized *de novo* from small metabolites.[2,3] The activation of these paths to pyrimidine synthesis depends on the cell type, its growth phase, and its developmental stage. In fully differentiated cells or in the resting stage, the rate of the *de novo* synthesis is low because the required pyrimidine level is met by the salvage pathway. In contrast, the rate of the *de novo* pyrimidine synthesis is high in proliferating cells in order to meet the increased demand for the precursors of DNA and RNA, along with other components.[5] Therefore, better understanding of the *de novo* activity of pyrimidine biosynthesis is necessary to elucidate the regulation of the growth-state-dependent control mechanisms of this pathway and their breakdown and failure in cancer.

De novo Pyrimidine Biosynthesis

The pyrimidine *de novo* biosynthetic pathway effectively serves the rapid growth of tumors.[2] It is carried out by six enzymatic steps to form Uridine 5'-monophosphate (UMP). The first three steps in pyrimidine *de novo* biosynthesis in mammalian cells are catalyzed by three enzymes, Carbamoyl-phosphate synthetase II (CPSase II), Aspartate

transcarbamoylase (ATCase), and Dihydroorotase (DHOase), referred to as CAD. These enzymatic activities are all carried on a single polypeptide chain that forms carbamoyl phosphate, carbamoyl aspartate, and dihydroorotate, respectively. These steps are chemotherapeutic targets, since they catalyze the first steps of the pathway. The rest of the pyrimidine pathway is catalyzed by dihydroorotate dehydrogenase (DHOdhase), UMP Synthase (UMPSase), and CTP synthase (CTPSase) to form orotate, UMP, and CTP, respectively (Figure 1).[6,7] CAD is the key regulatory enzyme in mammalian *de novo* pyrimidine biosynthesis because it catalyzes the first rate limiting step of the pathway.

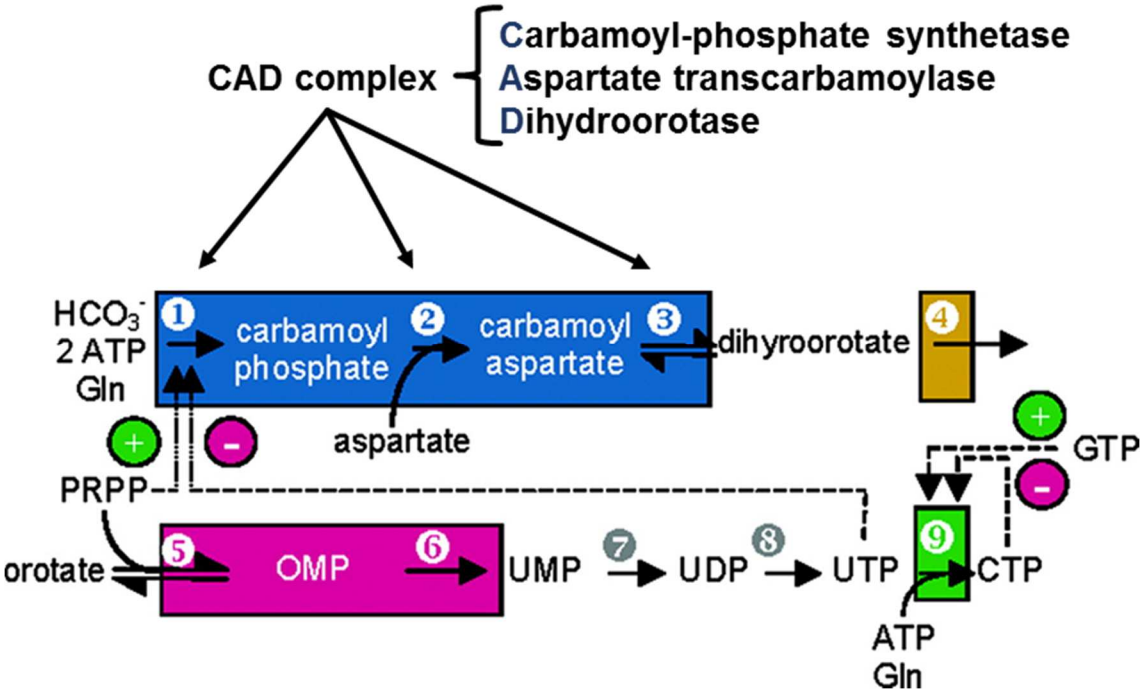

Figure 1: The *de novo* pyrimidine biosynthetic pathway.[3]

Aquifex aeolicus

A. aeolicus belongs to the Aquificales order, and is gram-negative with no capability to form spores. Aquificales are hyperthermophilic bacteria that live in hot springs, both

terrestrial and marine. Aquificales are autotrophs as they can use inorganic substances to form nutritional organic substances.[8] *A. aeolicus* is an extreme hyperthermophilic organism with an ancient lineage. This bacteria grows in temperatures reaching up to 95°C, in a CO_2, O_2, and H_2 atmosphere.[9] This property gives the enzymes from *A. aeolicus* great stability in the face of changes in temperature, pressure, and levels of O_2. This stability is an attractive feature for research studies involving enzyme activity.

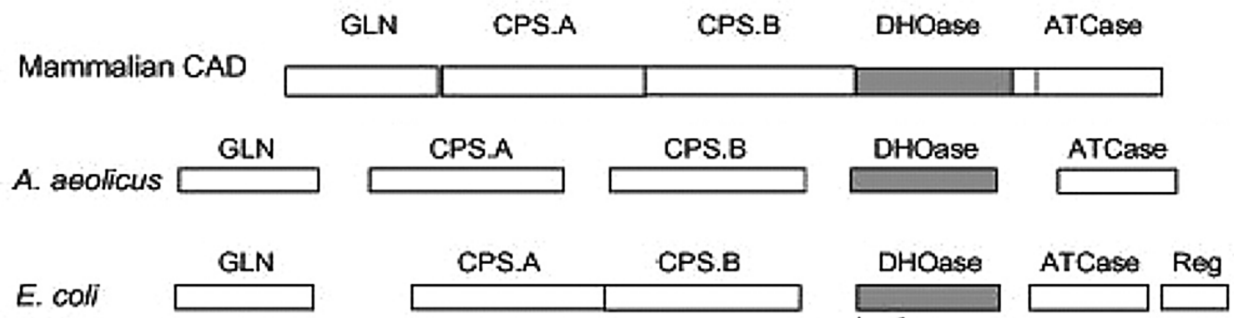

Figure 2: Comparison of the structural organization of the enzymes catalyzing the first three steps of the *de novo* pyrimidine biosynthesis in mammals, *A. aeolicus,* and *E. coli.*[11]

CAD Complex vs. *Aquifex aeolicus* Enzymes

The first three steps in *de novo* pyrimidine biosynthesis in mammals are catalyzed by CAD.[2,3] In prokaryotic cells, the enzymes involved in the pathway are encoded by separate genes and have separate expressions. These enzymes can function independently, such as in *E.coli*, or can be associated with a multifunctional complex as in the case of *A. aeolicus* (Figure 2).[10] The latter is similar in function to the mammalian complex. Unlike the mammalian enzymes, the first three enzymes in the *de novo* pyrimidine biosynthesis in *A. aeolicus* are monofunctional proteins. Furthermore, unlike

the mammalian system, the first step catalyzed by the bacterial CPSase is not the committed step as it catalyzes the formation of carbamoyl phosphate for both pyrimidine and arginine biosynthesis.[12] Therefore, the function of the second enzyme ATCase is likely to be the first committed step in pyrimidine biosynthesis in *A. aeolicus* to catalyze the formation of carbamoyl aspartate.[3,12] The third enzyme DHOase catalyzes the reversible step to form dihydroorotate from carbamoyl aspartate. This activity is typically 10 fold lower than that of ATCase.

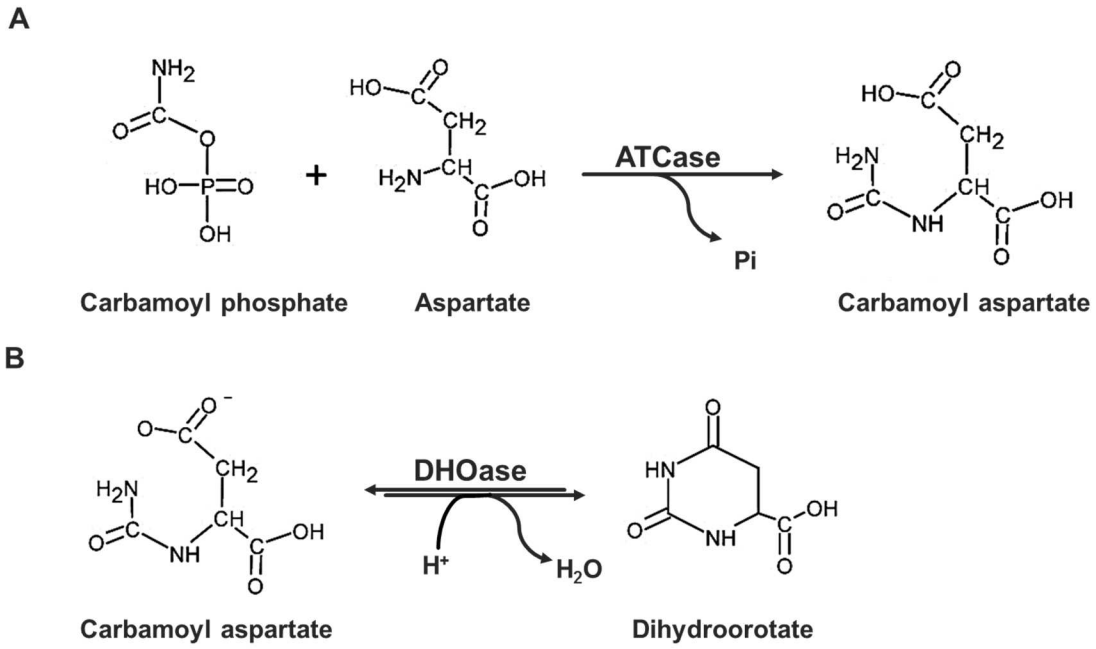

Figure 3: The second and third steps in pyrimidine biosynthesis. (A) ATCase catalyzes the condensation of carbamoyl phosphate and aspartate to form carbamoyl aspartate and phosphate. (B) DHOase catalyzes the formation of dihydroorotate and water from carbamoyl aspartate and H^+.[11,13]

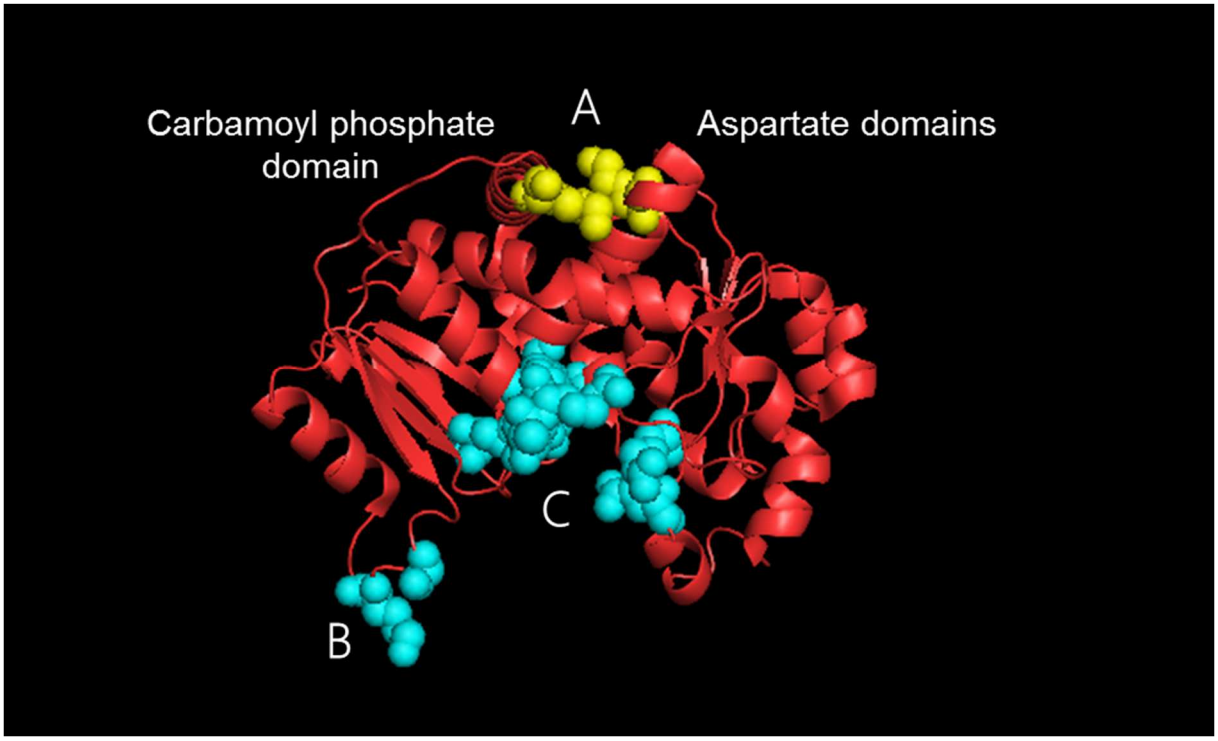

Figure 4: ATCase structure. (A) The residues at the interface between the carbamoyl phosphate and aspartate domains (Lys 26 and Lys 138, *yellow, space filled*) are shown. (B) A major residue for the two substrate binding (Lys 75, *blue, space filled*) is shown. (C) The active site residues (Gln 219, Val 190, Phe 191, Leu 8, Gly 122, and Phe 103, *blue, space filled*) are shown. This figure was prepared using PyMol viewer (PDB Id: 3B6N).[13]

Aspartate Transcarbamoylase in *Aquifex aeolicus*

ATCase catalyzes the formation of carbamoyl aspartate in the second step of pyrimidine biosynthesis (Figure 3.A). ATCase in bacteria is classified into three groups based on the number of subunits and the molecular mass. Class A is defined by the association of two trimers and six DHOase monomers to form 480-kDa dodecamers, e.g., *Pseudomonas aeruginosa* ATCase. In class B, there is association of two trimers

and three regulatory dimers to form 310-kDa dodecamers, e.g., *E. coli* ATCase. Class C is usually characterized by 100-kDa trimers, e.g., *Bacillus subtilis.*[13] Interestingly, ATCase in *A. aeolicus* differs from these classifications. *A. aeolicus* ATCase, a 34-kDa subunit, is encoded by the gene *pyrB*. ATCase has two domains, namely, carbamoyl phosphate and aspartate, connected internally through Lys 26 and Lys 138 (Figure 4). ATCase in *A. aeolicus* is inactive as a monomer, and only functions when it forms a trimer.[13]

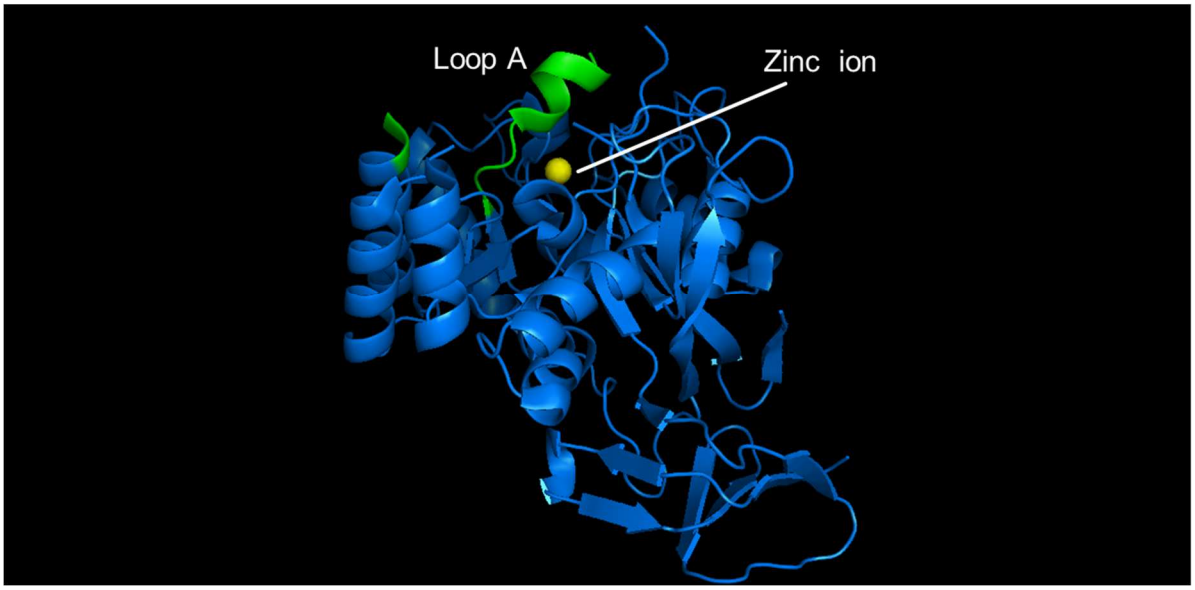

Figure 5: The structure of *A. aeolicus* DHOase. It is an inactive monomer presumably due to the intrinsically disordered loop (Loop A, *green*) blocking any access to the active site. DHOase has a single zinc ion (*yellow*). This figure has been prepared using the PyMol viewer (PDB Id: 1XRF).

Dihydroorotase Structure in *Aquifex aeolicus*

The first crystal structure of *A. aeolicus* DHOase allows its classification as a type I dihydroorotase.[14] This classification is based on the number of zinc ions and their

function in DHOase, which is same as the DHOase domain in the mammalian CAD.[3,14] The sequence homology between the DHOase domain of the mammalian CAD and *A. aeolicus* DHOase is about 26% .[11,14] This homology is higher, between the DHOase in *Aquifex aeolicus* and mammalian CAD, than that found when compared to other bacteria. For example, *E. coli* [15] DHOase has13% sequence homology with the DHOase domain of CAD.[11,14] These similarities demonstrate that *Aquifex aeolicus* can be used as a model system to study the enzymes involved in *de novo* pyrimidine biosynthesis.

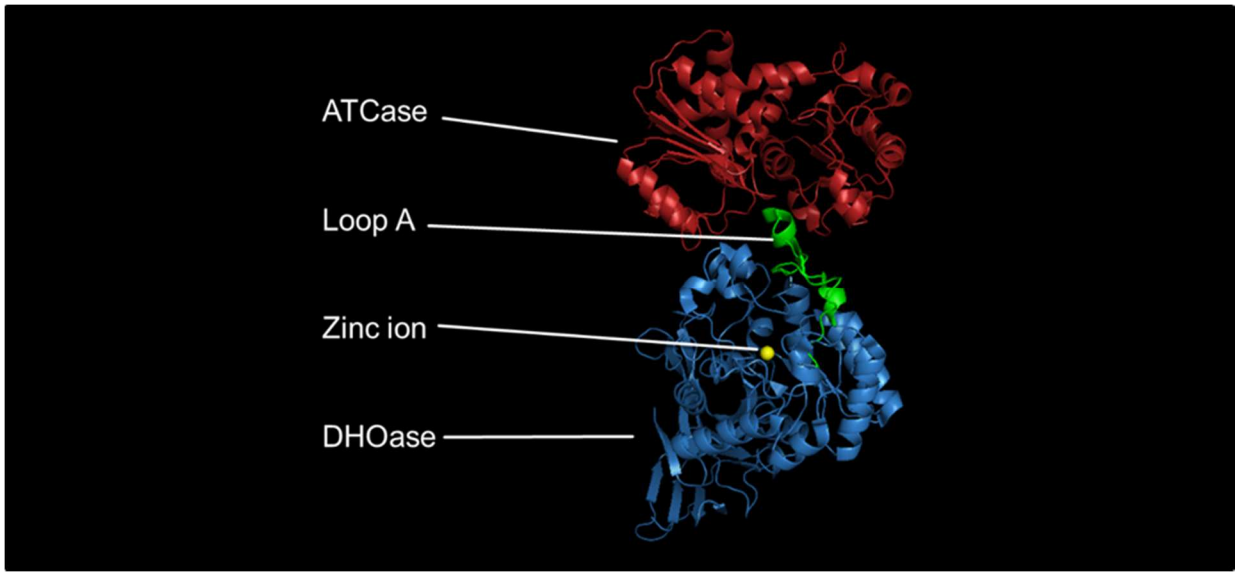

Figure 6: One ATCase monomer complexed with one DHOase monomer of the dodecameric DHO-ATC complex (DAC).

DHO – ATC Complex

The first crystal structure of the dodecameric complex of dihydroorotase and aspartate transcarbamoylase from *A. aeolicus* was solved in 2009.[10] This structure is predicted to be a possible model of mammalian CAD since it is the first structure of a multienzyme complex in the pyrimidine pathway.[10,11,14] Also, the active site of DHOase

in *A. aeolicus* has only one zinc atom, Znα. This zinc atom shows a square-pyramidal geometry with four amino acid residues: His-61, His-63, Asp-153, Asp-305, and one water molecule, all as ligands.[11,14] Moreover, the metal binding signature sequence is exactly the same as in CAD and differs by only one residue in *E. coli.* Although there is a second zinc site, the absence of the second zinc ion does not seem to affect the reversible reaction of carbamoyl aspartate to form dihydroorotate (Figure 3.B). Thus, DHOase is activated by a mononuclear metal ion.[15,16] Nevertheless, the DHOase in *A. aeolicus* is inactive and only becomes active on association with ATCase, despite the binding of the zinc.[11,14] There are three factors which may explain why the isolated enzyme DHOase in *A. aeolicus*, is inactive (Figure 5). First, there is no access to the active site because of the bond between the Znα and Cys181. This blocking interaction is not found in the DHOase in *E.coli*. Second, it may be because of the absence of the second zinc atom in DHOase in *A. aeolicus,* although recent studies suggest that it is not essential for catalytic activity.[16] Third, there are three loops that have intrinsic disorders around the active site that are likely blocking any access to it.[10] The importance of these three factors is highlighted in the structure of the stoichiometric complex of DHOase associating with ATCase in *A. aeolicus*.[10] The complex is a hetero dodecamer that forms an unfilled space or cavity on the inside. The ATCase – DHOase complex (DAC) is formed by two trimers of ATCase and three dimers of DHOase enzymes, 12 enzymes in total, where all the active sites are facing the internal, aqueous phase. This specific organization appears to facilitate the interaction between the active sites and activates the DHOase in order to catalyze the third step in the *de novo* pyrimidine biosynthetic pathway that results in the formation of dihydroorotate.[10] Upon complex formation,

Loop A of DHOase interacts with the ATCase domain rendering the DHOase active site accessible (Figure 6).[17]

Importance of Loop A

Recently, enzyme assays were conducted to determine the binding affinities of synthetic peptides from certain regions of loop A to DAC in *A. aeolicus*.[17] The peptides were used in different concentrations to determine the stoichiometry of the peptide-protein complex. The results indicated that the peptide, NEGEVSALLGLS, inhibited the functional interaction of DAC in an allosteric manner. This peptide, which is part of loop A, was shown to alter the catalytic activities of the DAC complex likely through the disruption of the interface between the DHOase and ATCase domains.[17] These results provided a promising lead on the potential of loop A as a noncompetitive drug target to control the second and third steps in *de novo* pyrimidine biosynthesis. The peptide, DHCEDDKLA, may serve as a competitive inhibitor because it may bind directly to the active site on the DHOase domain. However, the competitive inhibitor function of this region of loop A has not been tested prior to this study.

Hypothesis

In loop A, residues 179 – 186 are involved in competitively inhibiting the DHOase active site while residues 192 – 203 noncompetitively inhibit the ATCase active site.

179 DHCEDDKLAYGVINEGEVSALLGLSSRAPEAE 210

Goals

1. To determine the function of specific residues of loop A in DAC functional interactions.
2. To alter the catalytic activities through disruption of the interface between the two enzymes from *A. aeolicus.*

CHAPTER 2: EXPERIMENTAL METHODS

Peptide Synthesis

The SPPS method was used to synthesize the peptide. 0.4 mmol amino acid, protected by *N*-α-fluorenylmethyloxycarbonyl (Fmoc), and 0.4 mmol activating agent hydroxylbenzotriazolyltetramethyluronium hexafluorophosphate (HBTU) (4X excess) were added into a vial. 0.1 mmol of *p*-methylbenzhydrylamine (MBHA) resin was used as the solid support to give a carboxamide terminus. The PS3 synthesizer was programmed to couple amino acids, remove each Fmoc group, and wash with *N,N*-dimethylformamide (DMF) at each step. In order to cleave the peptide from the resin, the peptide was treated by adding 0.5 mL distilled water, 0.5 mL phenol scavenger, and 10 mL trifluororacetic acid (TFA). The peptide resin was stirred for two hours at room temperature. The peptide-containing solution was then removed from the resin through filtration, following which cold diethyl ether was added for peptide precipitation. The precipitant, the solid peptide, was collected by filtration and then dissolved in 35% ACN/H_2O and lyophilized. The peptides were dissolved in methanol first, and then the resultant solution was purified by reverse-phase high performance liquid chromatography (RP-HPLC) using an absorbance wavelength of 214 nm for detection. The peptide solution was injected and run with linear gradient of 10 – 50% ACN in H_2O over two hours. The solution was collected in test tubes where peaks were observed. The tubes containing pure peptide were combined and lyophilized before the purity was confirmed by RP-HPLC. Electrospray ionization mass spectrometry (ESI-MS) was used to confirm the molecular weight of the peptides. The resultant peptides were dissolved in 100% dimethyl sulfoxide (DMSO) with a final concentration of 2 mg/mL.

Protein Expression

The *pyrB* and *pyrC* genes encoding *A. aeolicus* ATCase and DHOase were cloned into an expression vector, pRSET, to purify the expressed protein with His-tag on a Nickel resin. 3 µL of the plasmids pAApyrB and pAApyrC were transformed in a vial with 40 µL of the competent cells (the *E. coli* strain BL21 (DE3*)) along with 5 µL of helper plasmid pSJS1240. The mixture was incubated in ice for 30 min. The *E. coli* were heat shocked for exactly 30 seconds in a 42°C water bath. 250 µL of pre-warmed SOC medium was added to the *E. coli* cells. The vials were placed in a shaker at 37°C, 220 rpm, for one hour. The transformed cells were placed on a pre-prepared LB agar plate containing 100 µg/mL ampicillin and 50 µg/mL spectinomycin, and grown at 37°C overnight. After growing the cells overnight, the cells were centrifuged at 13,000 rpm at 4°C for 30 min. The medium was discarded and the pellets were re-suspended in 3 mL of 50 mM Tris/Cl buffer. Sonication was applied to disrupt the cells 6 times for 30 seconds. The extracted cells were centrifuged at 13,000 rpm at 4°C for 30 min.

The recombinant protein was purified by Ni^{2+} affinity chromatography as the proteins were expressed with a His tag. The supernatant was applied to a 1 mL Ni^{2+}-ProBond column equilibrated with 50 mM Tris-HCl and 200 mM NaCl (TN buffer). The proteins were eluted with successive 1 mL aliquots of increasing concentrations of imidazole from 50 to 400 mM in TN buffer and the fractions were collected. Analysis of the fractions was accomplished by Sodium dodecyl sulphate-polyacrylamide gel electrophoresis (SDS-PAGE) with 10% acrylamide. Fractions containing pure *A. aeolicus* ATCase and DHOase were applied to the bicinchoninic acid (BCA) assay kit to determine protein concentration.

Enzyme Assays

For the ATCase assay, the enzyme activity was measured by a colorimetric method where the assay was performed as a function of enzyme concentration. The samples were prepared by adding 500 µL of assay buffer (3 ml of 0.5 M Tris, 0.25 mL aspartate, and H_2O up to15 mL), enzyme (two assays, ATCase only and ATCase in DAC, ATC-DHO, 2:3 ratio), and H_2O up to 1 mL in culture tubes. The sample reactions were initiated by adding the substrate (100 µL of 50 mM carbamoyl phosphate), mixed and placed in a 70°C water bath. The total assay time was 3 min. After 3 min, 1 mL of 5% acetic acid was added to quench the reaction, followed by mixing and placement at room temperature. 2 mL of color mix (antipyrine and monooxime, 1:2 ratio) was added to each tube, which acted as an indicator for the product carbamoyl aspartate. Absorbance at 466 nm of carbamoyl aspartate was measured after 60 min incubation at 60°C. Another ATCase assay was performed as a function of peptide concentration. The peptides DHCEDDKLA and NEGEVSALLGLS were added at different concentrations.

For DHOase, the assay was performed as a function of enzyme concentration. The samples were prepared by adding 500 µL of assay buffer (0.1 M Tris), enzymes (DAC, ATC-DHO, 2:3 ratio), and H_2O up to 1 ml in culture tubes. The sample reactions were initiated by adding the substrate (50 µL of 80 mM dihydroorotate), mixed and placed in a 70°C water bath. The assay proceeded as has been described in the ATCase assay section.

In all assays, the concentration of carbamoyl aspartate was calculated from standard curves created with known concentrations of 10 mM carbamoyl aspartate. The data plot is linear.

PyMol Viewer

Enzyme structures were visualized and modeled by the PyMol viewer software. First, the structure was downloaded from a protein data bank website as a PDB File (Text). From the PyMol molecular graphics system window, the sequence was displayed in order to select the desired residues. The sequence appeared on the top of the PyMol viewer window. Different commands (Action, Show, Hide, Label, and Color) from the PyMol Names Panel were used to make the desired changes to the structure. The desired residues within specific distances were selected. On the structure (the selected residues are marked), the “actions” option appeared on a right-click of the mouse. The following options were used: “around” and “residues within 4, 5, and 6 Å”

CHAPTER 3: RESULTS AND DISCUSSION

Loop A, part of DHOase, has been reported as a significant loop by which DHOase and ATCase activities are functionally coupled, and loop A appeared to be wedged between the two ATCase domains. The residues of loop A are believed to have separate effects based on the location of these residues. It is critical to identify the specific function of these residues in order to potentially regulate the enzyme activity with greater control. Moreover, the specific function can be identified by determining where and how specific parts of loop A bind to specific regions between these two enzymes (Figure 7).

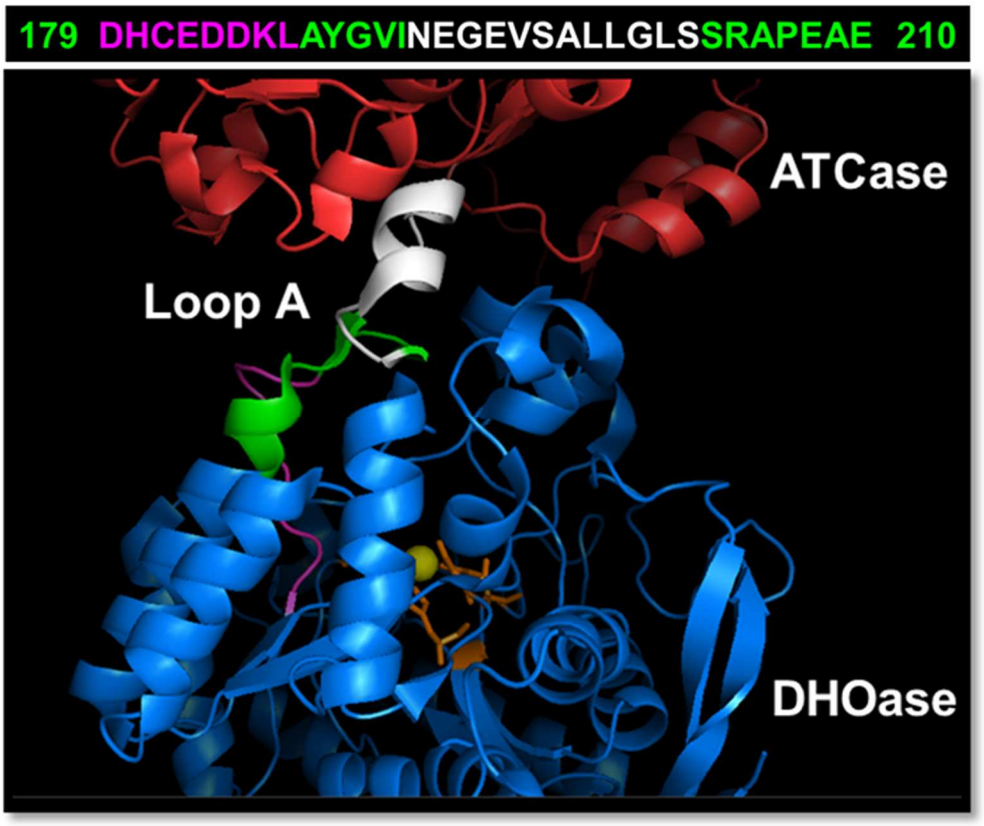

Figure 7: Loop A of DHOase. The sequence of loop A (*top*) in different colors corresponds to those in the structure (*bottom*).

The peptides HCE, DHCEDD, DHCEDDKLA, and NEGEVSALLGLS were prepared using the PS3 synthesizer with high purity of 99 to 100% after purification. The purification of the peptides was confirmed by RP-HPLC. The peptide yield on SPPS is generally around 20 to 50%, and different yield percentages were obtained experimentally (Table 1). The peptides were identified by ESI-MS and dissolved in DMSO with a final concentration of 2 mg/mL.

Table 1: Synthetic peptide yields

Peptide	**Percent yield**
HCE	31 %
DHCEDD	33 %
DHCEDDKLA	48 %
NEGEVSALLGLS	25 %

The *A. aeolicus* ATCase protein was expressed in *E. coli* BL21 (DE3*) and purified using Ni^{2+} affinity chromatography. Subsequent to extensive washing, about 2/3 of the ATCase protein was eluted with 200 mM imidazole/TN buffer and a third was eluted with 300 mM imidazole/TN buffer. The molecular mass of the purified ATCase corresponded to 34-kDa as compared to the protein ladder, a reference to determine the mass of the unknown protein (Figure 8).

The DHOase protein from *A. aeolicus* was expressed in *E. coli* BL21 (DE3*). The purification was accomplished by Ni^{2+} affinity chromatography. About 75% of the protein was eluted with 200 mM imidazole/TN buffer and the rest of the total protein

was eluted with 300 mM imidazole/TN buffer. As compared to the ladder, the molecular mass corresponded to that reported in the literature, 46-kDa (Figure 9).

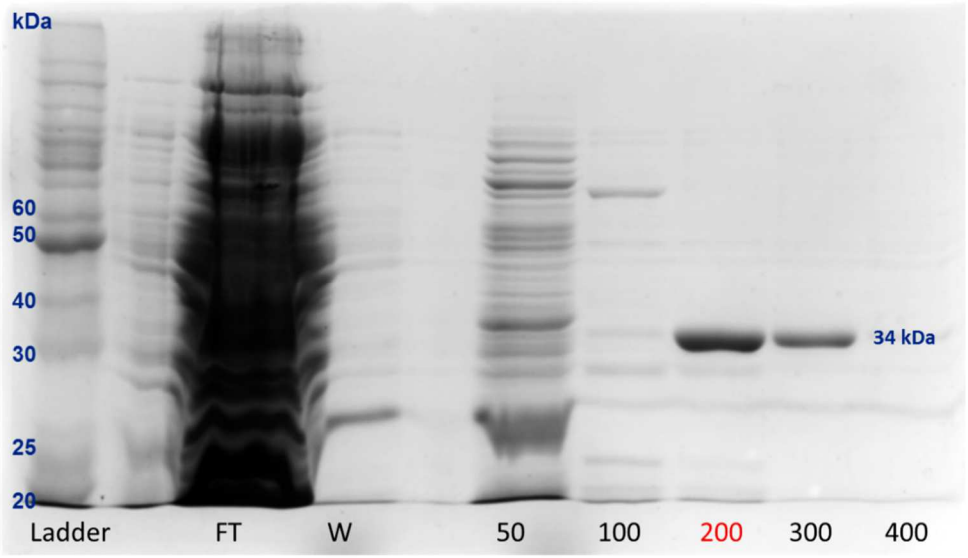

Figure 8: SDS-PAGE gel of *A. aeolicus* ATCase expression, purified by Ni^{2+} affinity chromatography.

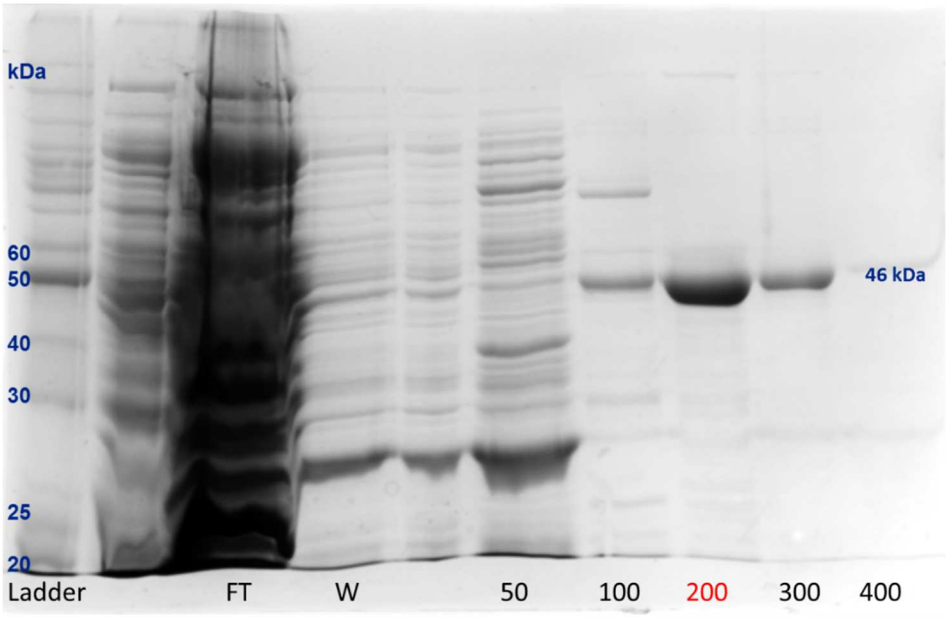

Figure 9: SDS-PAGE gel of *A. aeolicus* DHOase expression, purified by Ni^{2+} affinity chromatography.

The effect of the peptide NEGEVSALLGLS has been reported previously as an allosteric noncompetitive inhibiter.[18] The peptide acted by mimicking the end segment of loop A in DHOase in order to diminish the interaction necessary with ATCase. Interestingly, the activity of the isolated ATCase subunit was more affected by the peptide NEGEVSALLGLS than the ATCase activity in DAC. The catalytic activity of both the ATCase and DHOase were affected (Figures 10, 11). Percent inhibition of the peptide was variable (Table 2), which helped raise several questions, such as: a) Which one of these enzymes is most affected by the peptides? b) How does the DAC complex modulate the effect of the peptides on the isolated enzymatic components? c) Which part of loop A affects only the ATCase or DHOase activities?

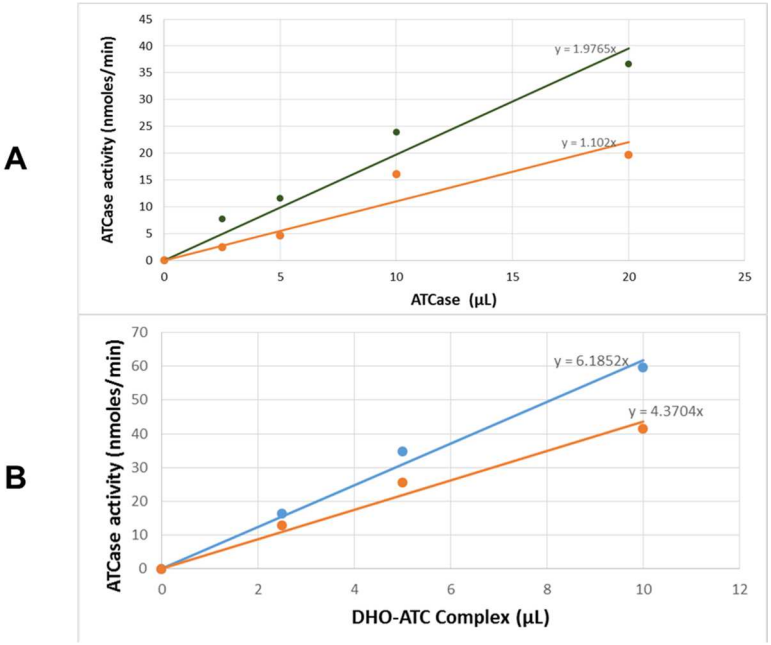

Figure 10: The ATCase assay and the effect of the peptide as a function of increasing enzyme concentration. The peptide used is NEGEVSALLGLS (*orange*) (A) The ATCase activity of the isolated ATCase subunit (*green*). (B) The ATCase activity of DAC (*blue*).

The effect of the peptides reflecting different regions of loop A on the activity of the isolated ATCase subunit was measured by measuring the ATCase activity. The enzymatic assay was performed at a variety of enzymes concentrations. Different peptides representing unique and/or overlapping regions of the first segment of loop A, residues 179 – 186, were synthesized (HCE, DHCEDD, DHCEDDKLA). In the case of all the peptides above, the effect on the isolated ATCase activity was not evident in the region of lower protein concentrations. No effect was observed upon the addition of the peptides (HCE, DHCEDD, DHCEDDKLA) to lower concentrations of the isolated ATCase domain (2.5 µL of 0.164 µg/mL) suggesting a concentration-dependence response to the peptides (Figure 12). Increasing the concentration of the protein, however, showed the inhibitory effect of the peptides on the isolated ATCase activity (Table 2).

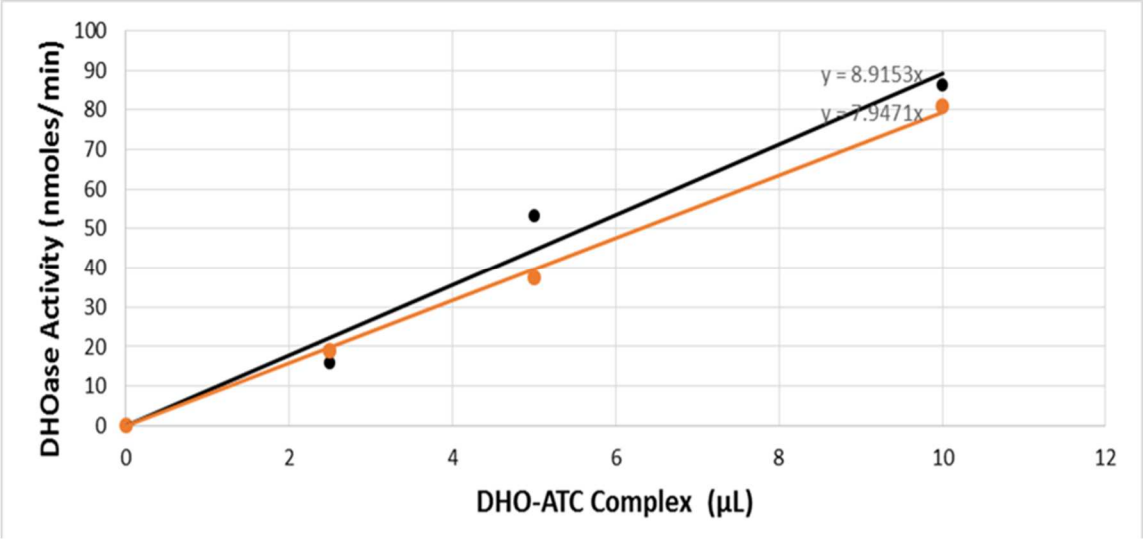

Figure 11: The DHOase activity inhibition of DAC as a function of increasing enzyme concentration. DHOase activity in the absence of peptide (*black*) and the presence of the peptide NEGEVSALLGLS (*orange*).

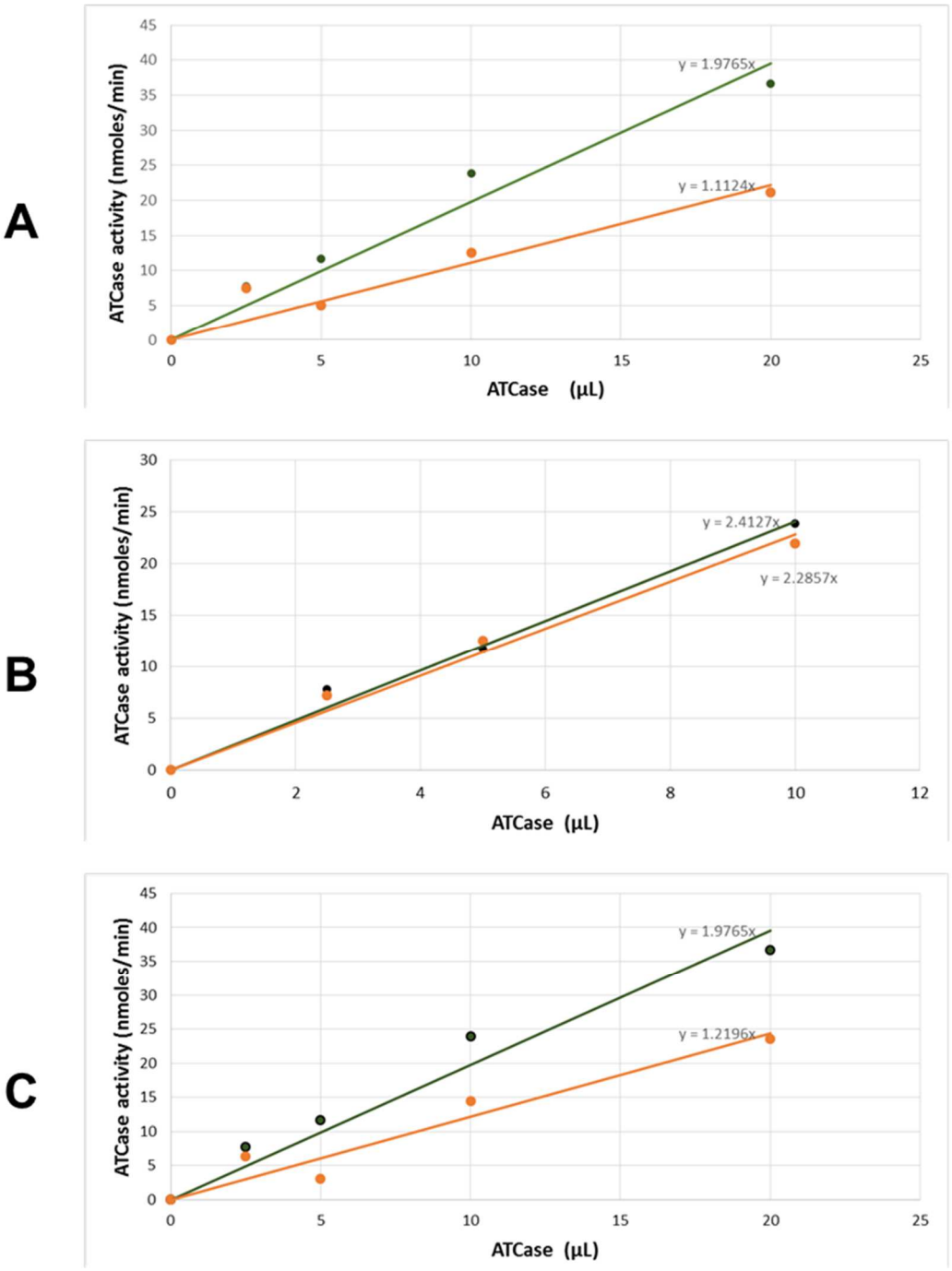

Figure 12: The activity of the isolated ATCase subunit as a function of increasing enzyme concentration. The isolated ATCase subunit activity (*green*) and the effect of different peptides (*orange*). (A) HCE peptide. (B) DHCEDD peptide. (C) DHCEDDKLA peptide.

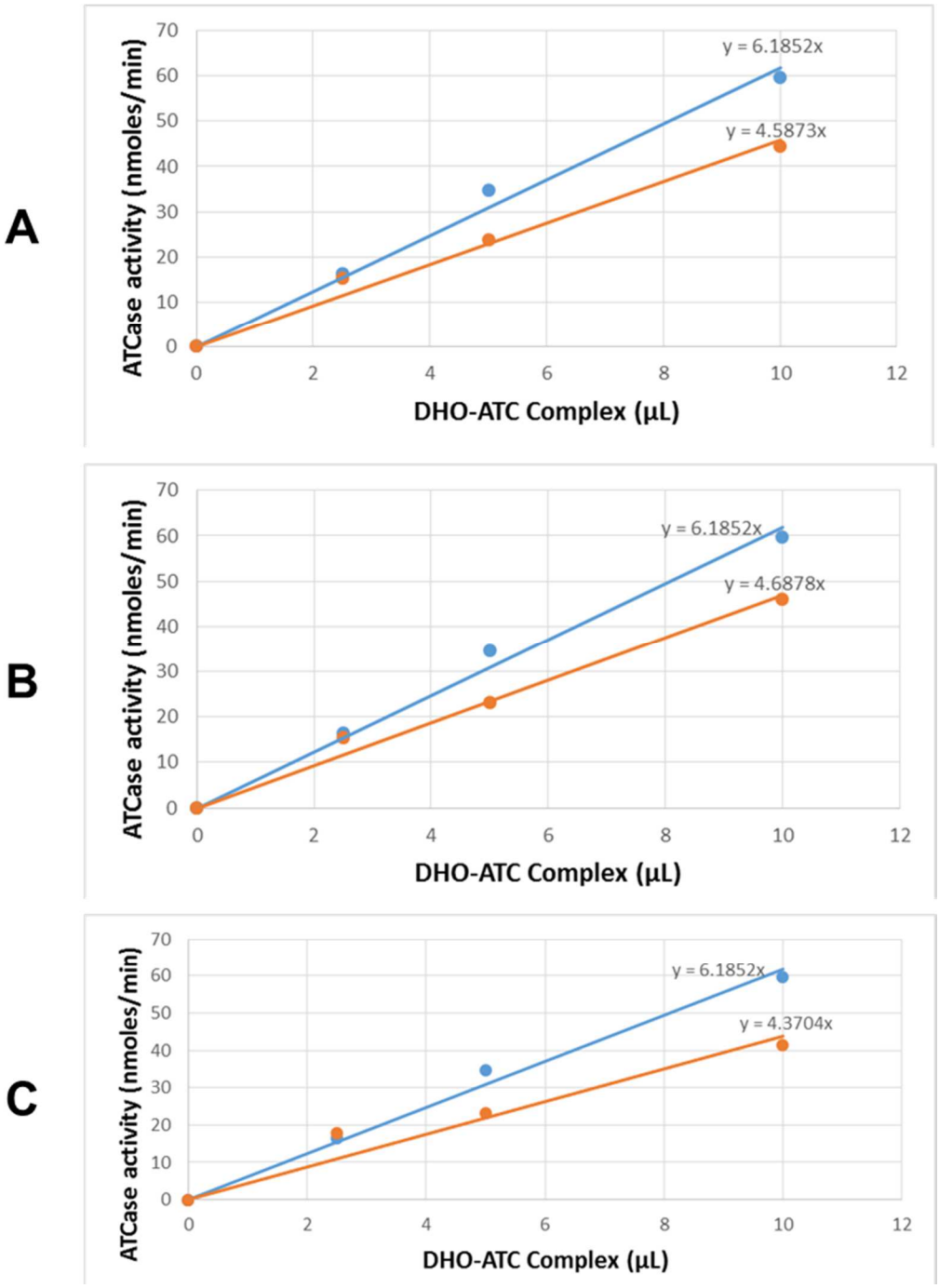

Figure 13: The ATCase activity of DAC inhibited by short peptides. The activity of ATCase of DAC (*blue*) and the effect of different peptides (*orange*) as a function of increasing enzyme concentration. (A) HCE peptide. (B) DHCEDD peptide. (C) DHCEDDKLA peptide.

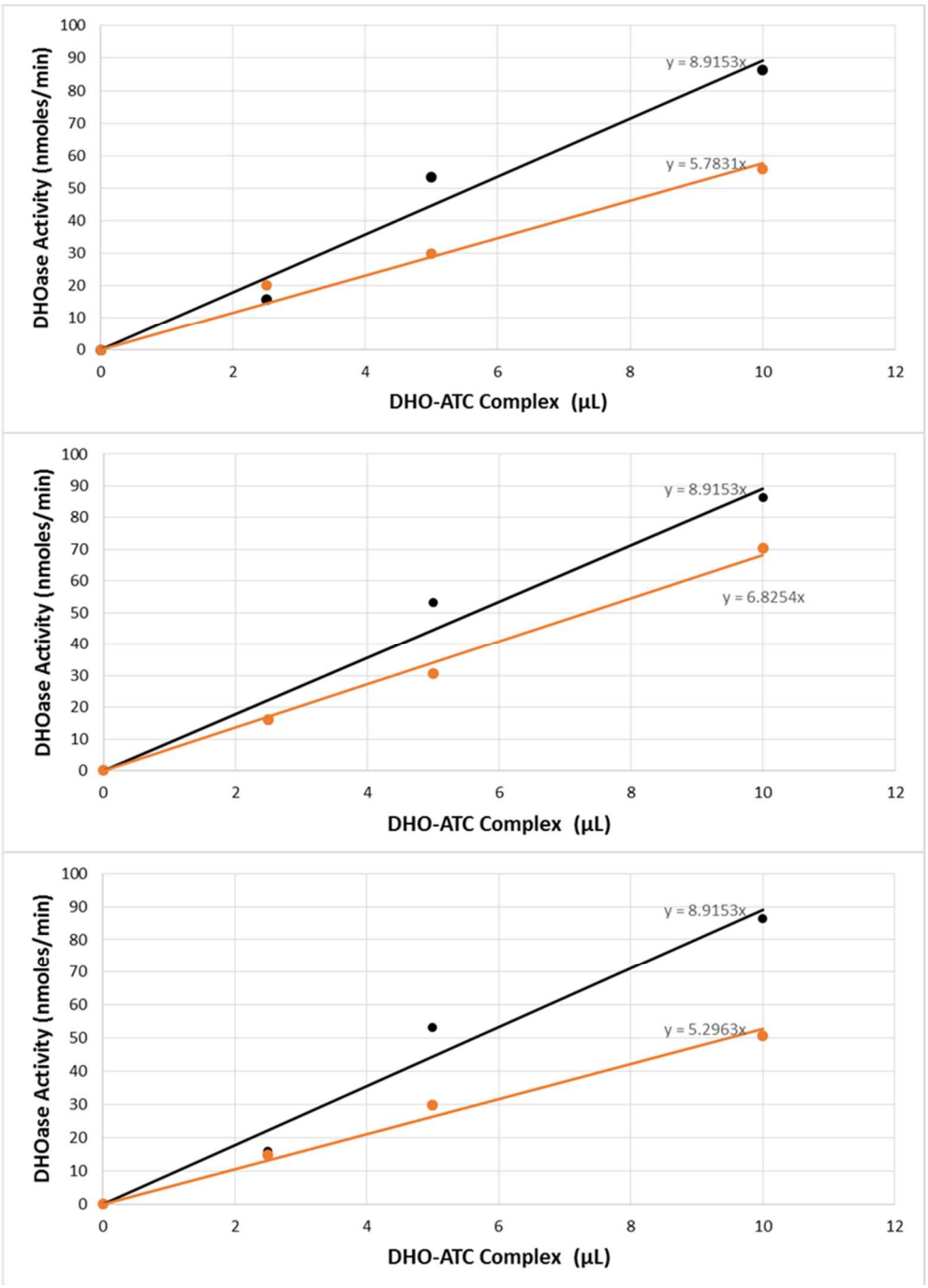

Figure 14: The DHOase activity of DAC inhibited by short peptides. The activity of DHOase of DAC (*black*) and the effect of different peptides (*orange*) as a function of increasing enzyme concentration. (A) HCE peptide. (B) DHCEDD peptide. (C) DHCEDDKLA peptide.

Similar percent inhibitions were observed for the peptides' effect on the activity of ATCase in the DAC complex. The DAC complex was prepared by the addition of 2.5 µL of (0.164 µg/µl) ATCase and (0.238 µg/µl) DHOase (2:3 ratio) and the peptides (with final concentration 0.2 mg/ml) were added (Figure 13). The percent inhibition of the ATCase activity in the DAC complex were found to be in the same range as in those observed with the isolated subunit.

The effects of the peptides, HCE, DHCEDD, DHCEDDKLA, on the activity of DHOase of DAC was measured starting at the lowest concentration, 2.5 µL of (0.164 µg/µL) ATCase/ (0.238 µg/µL) DHOase (2:3 ratio), and with increasing enzyme concentration (Figure 14). The effects are similar to those found on the ATCase activity of DAC; however, the percent inhibition on DHOase of DAC activities varies between these peptides, which reflects the effect of the specific residues on the DHOase activity of DAC.

Table 2: Peptides effect (inhibition %) on the isolated ATCase subunit, ATCase of DAC, and DHOase of DAC.

Peptide	**ATCase activity inhibition % (ATCase)**	**ATCase activity inhibition % (DAC)**	**DHOase activity inhibition % (DAC)**
HCE	43.7	25.8	35.1
DHCEDD	5.26	24.2	23.4
DHCEDDKLA	38.3	29.3	40.6
NEGEVSALLGLS	44.2	29.3	10.9

A

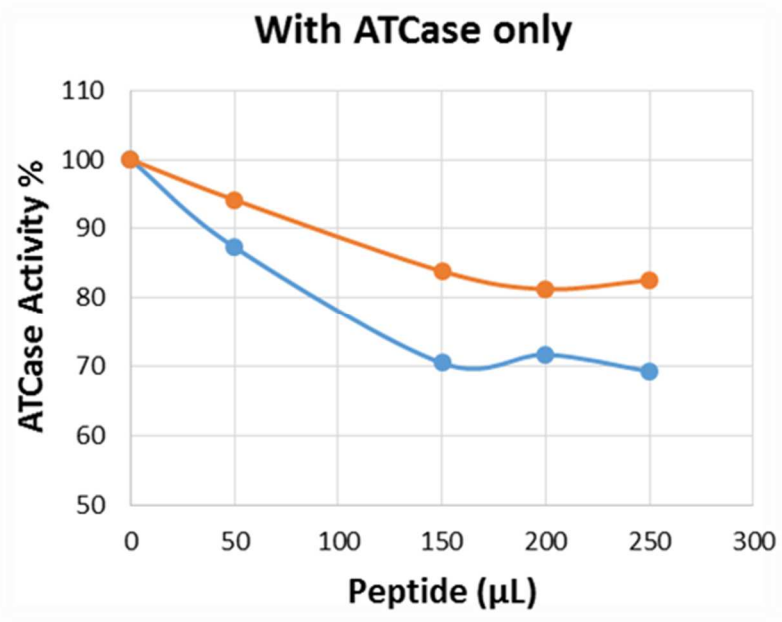

B

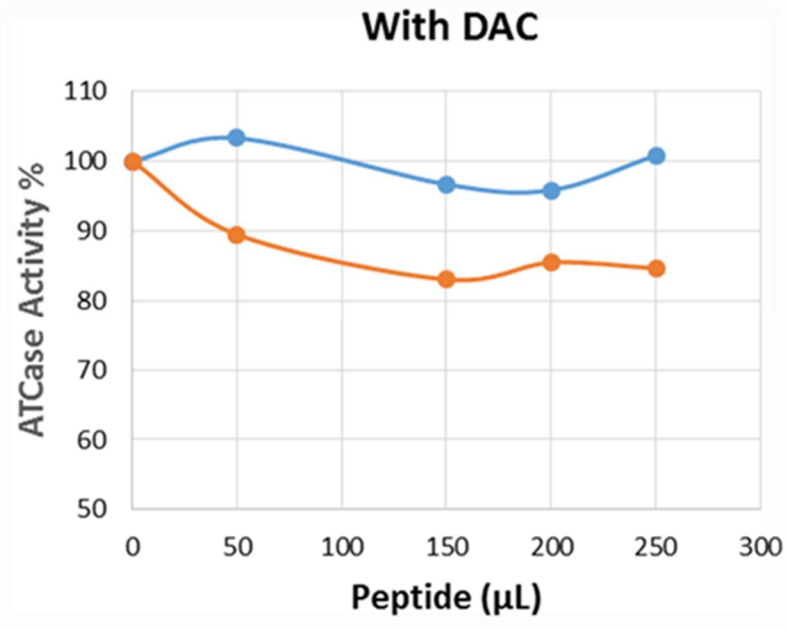

Figure 15: Percent of ATCase activity as a function of increasing peptide concentration. The effect of the peptides NEGEVSALLGLS (*orange*) and DHCEDDKLA (*blue*) was determined (A) The ATCase activity of the isolated ATCase subunit. (B) The ATCase activity of DAC.

The effect on the ATCase activity of increasing peptide concentration (0.1, 0.3, 0.4, and 0.5 mg/mL) was different between the isolated ATCase subunit activity and the ATCase activity of DAC. The peptide, DHCEDDKLA, affects the isolated ATCase subunit activity more than the peptide, NEGEVSALLGLS. The ATC activity of DAC with NEGEVSALLGLS, however, has more of a dependence upon the peptide concentration as compared to the effect of the peptide, DHCEDDKLA, which does not seem to have a significant effect on the ATCase activity of DAC (Figure 15).

All of the results are summarized in Tables 3 and 4.

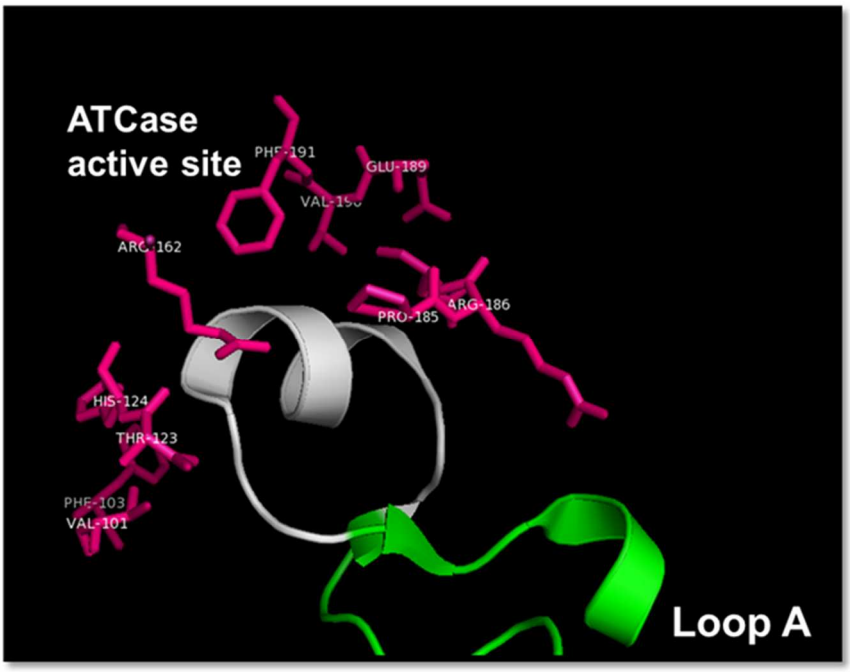

Figure 16: The residues of the ATCase active site interacting with part of loop A, NEGEVSALLGLS (*white*).

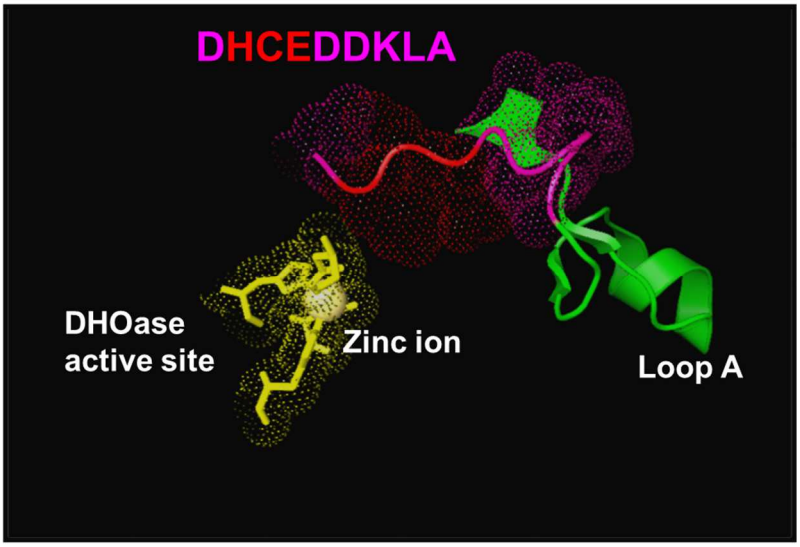

Figure 17: Part of loop A interaction with the metal binding residues in the DHOase.

Table 3: Peptide effect on ATCase activity.

Peptide	ATCase inhibition % (alone)	ATCase inhibition % (DAC)	Data Interpretation
HCE	43.7	25.8	• DHOase is protecting against the inhibition of ATCase by HCE • It might be a concentration dependence
DHCEDD	5.26	24.2	• DHCEDD is poor inhibitor of ATCase alone but not in DAC • The effect could be due to inhibition of DHOase
DHCEDDKLA	38.3	29.3	• The extra residues KLA are important in restoring the inhibition by HCE • The negative charge of D's is not inhibiting
NEGEVSALLGLS	44.2	29.3	• Inhibits ATCase non-competitively • DHOase protects ATCase from the inhibition • It might be a concentration dependence

Table 4: Peptide effect on DHOase activity.

Peptide	DHOase inhibition % (DAC)	Data Interpretation
HCE	35.1	• The peptide HCE inhibits DHOase • HCE is the minimum region needed to inhibit the DHOase
DHCEDD	23.4	• It is possible that DHCEDD inhibits DHOase which explain the inhibition of ATCase in DAC
DHCEDDKLA	40.6	• The positive region K increase the inhibition of DHOase
NEGEVSALLGLS	10.9	• The inhibition might be indirect, through ATCase inhibition, with a small effect on DHOase inhibition

CHAPTER 4: CONCLUSIONS AND RECOMMENDATIONS

The DHOase appears to be protective against the inhibition of ATCase by HCE, and it might be a concentration dependent effect. DHCEDD is a poor inhibitor of ATCase alone, but not in DAC. The effect could be due to the inhibition of DHOase. The extra residues, KLA, are important in restoring the inhibition by HCE. The negative charge of the D residues is not inhibiting. Moreover, the peptide HCE inhibits DHOase. HCE is the minimum region needed to inhibit the DHOase. It is possible that DHCEDD inhibits DHOase, which explains the inhibition of ATCase in DAC. The positive region provided by K increases the inhibition of DHOase. Additionally, the peptide NEGEVSALLGLS inhibits ATCase non-competitively and DHOase protects ATCase from this inhibition. The inhibition of DHOase activity of DAC by NEGEVSALLGLS might be indirect, through ATCase inhibition, with small effects on DHOase inhibition (Tables 3 and 4).

Further studies are needed to confirm these results. These may be achieved by performing dihydroorotate saturation curves with and without peptides, specifically HCE, to calculate and observe the effect on K_m. Also, it is crucial to find the minimum sequence of NEGEVSALLGLS that can serve as a non-competitive inhibitor with high affinity. It is important to construct DHCEDDKLA with changes in HCE and mutate HCE one residue at a time.

Proposed peptides for future work are suggested as follows: (a) residues that interact with the ATCase active site (Figure 16); GEVSALLG at 4 Å, EGEVSALLGL at

5 Å, and EGEVSALLGLS at 6 Å, (b) residues at the DHOase active site (Figure17); D*CEDDKLA, DH*EDDKLA, and DHC*DDKLA (where * is a mutant residue).

REFERENCES

1. http://www.cancer.org American Cancer Society http://www.cancer.org/research/cancerfactsstatistics
2. Hashimoto, M.; Morales, J.; Fukai, Y.; Suzuki, S.; Takamiya, S.; Tsubouchi, A.; Inoue, S.; Inoue, M.; Kita, K.; Harada, S.; et al. Critical Importance of the de Novo Pyrimidine Biosynthesis Pathway for Trypanosoma Cruzi Growth in the Mammalian Host Cell Cytoplasm. *Biochemical and Biophysical Research Communications* **2012**, *417*, 1002–1006.
3. Evans, D. R.; Guy, H. I. Mammalian Pyrimidine Biosynthesis: Fresh Insights into an Ancient Pathway. *Journal of Biological Chemistry* **2004**, *279*, 33035–33038.
4. Lu, C.; Li, A. P. *Enzyme Inhibition in Drug Discovery and Development: The Good and the Bad*; John Wiley & Sons, 2010.
5. Fairbanks, L. D.; Bofill, M.; Ruckemann, K.; Simmonds, H. A. Importance of Ribonucleotide Availability to Proliferating T-Lymphocytes from Healthy Humans Disproportionate Expansion of Pyrimidine Pools and Contrasting Effects of *De Novo* Synthesis Inhibitors. *J. Biol. Chem.* **1995**, *270* (50), 29682–29689.
6. Grayson, D. R.; Evans, D. R. The Isolation and Characterization of the Aspartate Transcarbamylase Domain of the Multifunctional Protein, CAD. *J. Biol. Chem.* **1983**, *258* (7), 4123–4129.
7. Qiu, Y.; Davidson, J. N. Substitutions in the Aspartate Transcarbamoylase Domain of Hamster CAD Disrupt Oligomeric Structure. *PNAS* **2000**, *97* (1), 97–102.

8. Lechner, M.; Nickel, A. I.; Wehner, S.; Riege, K.; Wieseke, N.; Beckmann, B. M.; Hartmann, R. K.; Marz, M. Genomewide Comparison and Novel ncRNAs of Aquificales. *BMC Genomics* **2014**, *15*, 522.
9. Guiral, M.; Tron, P.; Belle, V.; Aubert, C.; Leger, C.; Guigliarelli, B.; Giudici-Orticoni, M.-T. Hyperthermostable and Oxygen Resistant Hydrogenases from a Hyperthermophilic Bacterium Aquifex Aeolicus: Physicochemical Properties. *Int. J. Hydrog. Energy* **2006**, *31*, 1424–1431.
10. Zhang, P.; Martin, P. D.; Purcarea, C.; Vaishnav, A.; Brunzelle, J. S.; Fernando, R.; Guy-Evans, H. I.; Evans, D. R.; Edwards, B. F. P. Dihydroorotase from the Hyperthermophile Aquifiex Aeolicus Is Activated by Stoichiometric Association with Aspartate Transcarbamoylase and Forms a One-Pot Reactor for Pyrimidine Biosynthesis. *Biochemistry* **2009**, *48* (4), 766–778.
11. Ahuja, A.; Purcarea, C.; Ebert, R.; Sadecki, S.; Guy, H. I.; Evans, D. R. Aquifex Aeolicus Dihydroorotase: Association with Aspartate Transcarbamoylase Switches On Catalytic Activity. *Journal of Biological Chemistry* **2004**, *279* (51), 53136–53144.
12. Ahuja, A. A Novel Carbamoyl-Phosphate Synthetase from Aquifex aeolicus. *Journal of Biological Chemistry* **2001**, *276*, 45694–45703.
13. Purcarea, C.; Ahuja, A.; Lu, T.; Kovari, L.; Guy, H. I.; Evans, D. R. Aquifex Aeolicus Aspartate Transcarbamoylase, an Enzyme Specialized for the Efficient Utilization of Unstable Carbamoyl Phosphate at Elevated Temperature. *J. Biol. Chem.* **2003**, *278* (52), 52924–52934.
14. Martin, P. D.; Purcarea, C.; Zhang, P.; Vaishnav, A.; Sadecki, S.; Guy-Evans, H. I.; Evans, D. R.; Edwards, B. F. P. The Crystal Structure of a Novel, Latent Dihydroorotase

from Aquifex Aeolicus at 1.7 Å Resolution. *Journal of Molecular Biology* **2005**, *348* (3), 535–547.

15. Thoden, J. B.; Phillips, G. N.; Neal, T. M.; Raushel, F. M.; Holden, H. M. Molecular Structure of Dihydroorotase: A Paradigm for Catalysis through the Use of a Binuclear Metal Center. *Biochemistry* **2001**, *40* (24), 6989–6997.
16. Edwards, B. F.; Fernando, R.; Martin, P. D.; Grimley, E.; Cordes, M.; Vaishnav, A.; Brunzelle, J. S.; Evans, H. G.; Evans, D. R. The Mononuclear Metal Center of Type-I Dihydroorotase from Aquifex Aeolicus. *BMC Biochemistry* **2013**, *14* (1), 36.
17. Evans, H. G.; Fernando, R.; Vaishnav, A.; Kotichukkala, M.; Heyl, D.; Martin, P. D.; Hachem, F.; Brunzelle, J. S.; Edwards, B. F. P.; Evans, D. R. Intersubunit Communication in the Dihydroorotase-Aspartate Transcarbamoylase Complex of *Aquifex Aeolicus*: Intersubunit Communication in a Pyrimidine Biosynthetic Complex. *Protein Science* **2014**, *23* (1), 100–109.